SMILE Winter Campaign

M.-T. Walach [ID],[1]★ Y. Soobiah,[2] J. A. Carter,[2] D. K. Whiter,[3] A. J. Kavanagh,[4] M. D. Hartinger,[5]
K. Oksavik [ID],[6,7] M. L. Salzano[5] and M. O. Archer[8]

[1]*Physics Department, Lancaster University, Lancaster, LA1 4YW, UK*
[2]*Department of Astronomy and Physics, University of Leicester, Leicester, LE1 7RH, UK*
[3]*Department of Physics and Astronomy, University of Southampton, Southampton, SO17 1BJ, UK*
[4]*British Antarctic Survey, Cambridge, CB3 0ET, UK*
[5]*Space Science Institute, Boulder, CO 80301, USA*
[6]*Department of Physics and Technology, University of Bergen, 5007 Bergen, Norway*
[7]*Department of Arctic Geophysics, University Centre in Svalbard, P.O. Box 156 N-9171 Longyearbyen, Norway*
[8]*Department of Physics, Imperial College London, London, SW7 2AZ, UK*

ABSTRACT

This white paper is highly topical as it relates to the upcoming solar wind magnetosphere ionosphere link explorer (SMILE) mission: SMILE is a joint mission between the European Space Agency and the Chinese Academy of Sciences and it aims to build a more complete understanding of the Sun–Earth connection by measuring the solar wind and its dynamic interaction with the magnetosphere. It is a fully funded mission with a projected launch in 2025. This paper outlines a plan for action for SMILE's first Northern hemisphere winter campaign using ground-based instruments. We outline open questions and which data and techniques can be employed to answer them. The science themes we discuss are: (i) Earth's magnetosheath, magnetopause, and magnetic cusp impact on the ionospheric cusp region; (ii) defining the relationship between auroral processes, solar wind, and magnetospheric drivers; (iii) understanding the interhemispheric properties of the Earth's magnetosphere–ionosphere system. We discuss open questions (different to the mission goals) which may be answered using existing ground-based instrumentation together with SMILE data to leverage the maximum scientific return of the mission during the first winter after launch. This paper acts as a resource for planning, and a call to collaborative action for the scientific community.

Key words: SMILE Science – Ground-based instrumentation – Future opportunities – Instrumentation – Data methods.

1 INTRODUCTION

The solar wind magnetosphere ionosphere link explorer mission (SMILE) is a joint mission between the European Space Agency and the Chinese Academy of Sciences (Branduardi-Raymont & Wang 2022). SMILE is a game changer in imaging capabilities, and in particular, the simultaneous X-ray imaging of the dayside magnetosheath via charge exchange (Cravens 1997) and the Northern hemisphere auroral oval's ultraviolet emission. SMILE will also observe plasma using the light ion analyser and the magnetic fields using magnetometers, in situ. During the Northern hemisphere winter of 2025–2026, and subsequent winters of the mission, SMILE has an unprecedented opportunity to nearly continuously observe the Northern hemisphere over an entire season. The polar night of prolonged darkness means that auroral observations from the ground are possible across several months. Ground-based optical instruments, such as auroral imagers and spectrographs, allow us to collect contextual and multiscale data. In combination with SMILE, the additional parameters that ground-based instrumentation can provide will make it possible to test a range of predictions related to various M-I coupling processes, which will underpin the SMILE goals and allow achieving secondary science goals as outlined below.

Incoherent (e.g. the new European Incoherent Scatter radar, EISCAT_3D) and coherent scatter radars (e.g. the Super Dual Auroral Radar Network, SuperDARN) will provide further contextual multiscale information. Furthermore, the time period considered here should cover solar maximum and the declining phase of solar cycle 25. The sunspots recorded during solar cycle maxima tend to coincide with an increase in solar activity such as coronal mass ejections and these in turn, lead to an increase in extreme geomagnetic activity (Owens et al. 2021). Observing the magnetosphere during solar maxima is therefore particularly exciting due to the likely increase in extreme geomagnetic activity. The time period of this winter campaign is expected to yield information which will address the top level science questions of SMILE '*What are the fundamental modes of the dayside solar wind/magnetosphere interaction?*', '*What defines the substorm cycle?*', and '*How do Coronal Mass Ejection (CME)-driven storms arise and what is their relationship to substorms?*'(Branduardi-Raymont & Wang 2022).

As outlined by table 1 in Carter et al. (2024), numerous ground-based instrumentations are available which can support the SMILE mission. However, data from ground-based observatories are not centrally stored, so advance planning will ensure a timely scientific

★ E-mail: m.walach@lancaster.ac.uk

return. This white paper aims to plan the scientific themes of the winter campaigns and how progress can be made with ground-based instrumentation and observatories. Whilst final SMILE orbits are yet unknown and may change, the right ascension of the ascending node will be very similar to current plans (e.g. planned SMILE orbital period ∼51 h; planned apogee is 20 Re ±2 Earth radii geocentric distance; planned perigee is above 5000 km altitude; planned inclination is 90 ± 27°; Branduardi-Raymont et al. 2018). We must be ready in case of an opportunity of observing the winter of 2025/26 and for subsequent winters. We call the community to action to join us in planning ahead collaboratively to enable the greatest possible scientific return.

2 GROUND-BASED INSTRUMENTATION

Many ground-based instruments have been built over the years and what we summarize here is not an exhaustive list [see Carter et al. (2024) for additional details].

All Sky Imagers (ASIs) are ground-based auroral cameras which operate during hours of darkness to observe auroral emission. Currently, the SMILE ASI will serve as a purposefully conjunctive network of instruments to observe the aurora from the ground. The SMILE ASI is an upgrade from the THEMIS-ASI. THEMIS ASI was measuring white light, but the SMILE ASI measures Red-Green-Blue emission. The additional change is that the network shrinks in the longitudinal direction by removing the extremes on the East and West, but extends North South with additional stations. This is to capture the substorm bulge better. RGB gives us an opportunity to make an energy estimate of the precipitation, and also the Red line can be compared to the open closed field line boundary estimate from SMILE's Ultraviolet Imager (UVI). Similarly to auroral imaging cameras, meridian scanning photometers also observe the aurora at various wavelengths. In this white paper, we are primarily concerned with the SMILE ASIs and the meridian scanning photometer located at the Kjell Henriksen Observatory on Svalbard due to its favourable location in observing cusp aurora.

SuperDARN measures the backscattered Doppler-shift from ionospheric field-aligned irregularities, which allows measuring ionospheric flows (e.g. Chisham et al. 2007). Normally, each SuperDARN radar consists of 16 antennas which transmit and receive, and four antennas which receive only in the interferometry array. In the conventional Common Time Program, which is used for generating convection maps, 16 discrete positions covering ≃ 50° in azimuth are scanned every couple of minutes (e.g. McWilliams et al. 2023). The SuperDARN radar network has expanded in capability and coverage over the last decades (e.g. Nishitani et al. 2019; Walach et al. 2022). Many of the decade-old systems are being upgraded by digital systems, such as the Borealis system (McWilliams et al. 2023). The new digital radars allow for pulse-imaging which improves resolution, as well as sampling rate. The new digital systems can image an entire field of view in 3.5 s, as opposed to minutes (McWilliams et al. 2023). This is a vast improvement and allows us to observe more details than ever before, e.g. at the crucial mesoscales which couple regions of geospace together (Archer et al. 2024). Furthermore, more SuperDARN radars have been built over the past decade, with more underway: the upgraded Hankasalmi Auroral Imaging Radar System (HAIRS) radar is scheduled to be deployed in the summer of 2024. HAIRS will oversee a field of view covering the auroral oval and cusp, making it perfectly placed to target our science themes. SuperDARN operates on an almost continuous schedule. Most of the SuperDARN operating schedule runs the Common Time mode which is ideal for convection mapping

but time for specific experiments can be requested. The digital radars have added capability as they can run several experiments at the same time.

Arrays of magnetometers exist all over the globe. Often, these are fluxgate magnetometers, which typically operate at 1 Hz and measure DC and lower frequency variations related to quasi-static currents and Pc3-5 ULF waves (e.g. Field Line Resonance or magnetopause surface waves). We also propose the use of search coil magnetometers (also known as induction coil magnetometers) from networks such as the Magnetic Induction Coil Array (MICA); these magnetometers are built to measure Pc1-2 band ULF waves and higher frequencies as well (e.g. EMIC or ECH waves).

EISCAT_3D is a new instrument which will provide highly complementary measurements to SMILE. It is the next generation of incoherent scatter radar, capable of imaging a volume of the ionosphere above northern Scandinavia within the auroral zone. It consists of three phased arrays: a transmit-receiver site at Skibotn in Norway; a receiver in Karasuvanto, Finland; and a receiver in Kaiseniemi, Sweden. The digital beam forming allows for multiple beams to be generated simultaneously, while the three sites generate intersecting beams to give fully 3D observations. Each beam provides a profile of the ionospheric plasma density, ion temperature and electron temperature, and line-of-sight ion velocity; the intersecting beams allow multiple vector measurements within the volume such that the mesoscale variation of the vector ion velocity and electric field can be sampled.

The EISCAT_3D radar is highly configurable, such that the user can design experiments with beams in a range of pointing directions; this defines the spatial resolution, which can be as small as 10s km in the horizontal direction and sub km resolution when using the interferometric capability at the main site (Huyghebaert et al. 2024). Rapid switching of beams will allow for different experiments to be operated simultaneously. For example, a tight configuration of beams could be used to study the detailed plasma structure, whilst alternating with a low elevation fan to explore the drift of structures in the larger ionospheric flow.

The lowest beam elevation of EISCAT_3D is 30°, such that the largest field of view could be a circle of 210 km radius in the E layer (which covers ∼ 3° of geographic latitude) and 520 km in the F layer (∼ 7°). In practice this would result in sparse spatial sampling, but this is a trade-off with this configuration generating the largest possible field-of-view. The geometry of the receiver sites would also limit the number of intersecting beams in this configuration.

EISCAT_3D will mostly operate in campaign mode, though there is a desire from the organization and wider scientific community to run in a more continuous mode if possible. The exact mode of operation of EISCAT_3D will depend on the requirement of the user or the particular common programme experiment mode that is operated and may depend on the prevailing geomagnetic conditions. There are many ways that EISCAT observations can be combined with SMILE to study magnetosphere–ionosphere coupling. For example, the imaging capability of SMILE, when combined with EISCAT_3D observations will enable multiscale observations of the aurora; large scale features can be probed at much smaller scales, with detailed analysis of the ionospheric electrodynamics. We discuss this further in the following sections.

3 CAMPAIGN THEMES

This campaign is planned with several science goals in mind to ensure maximum scientific output and return. Each campaign theme requires different observing capabilities. The following figures show example
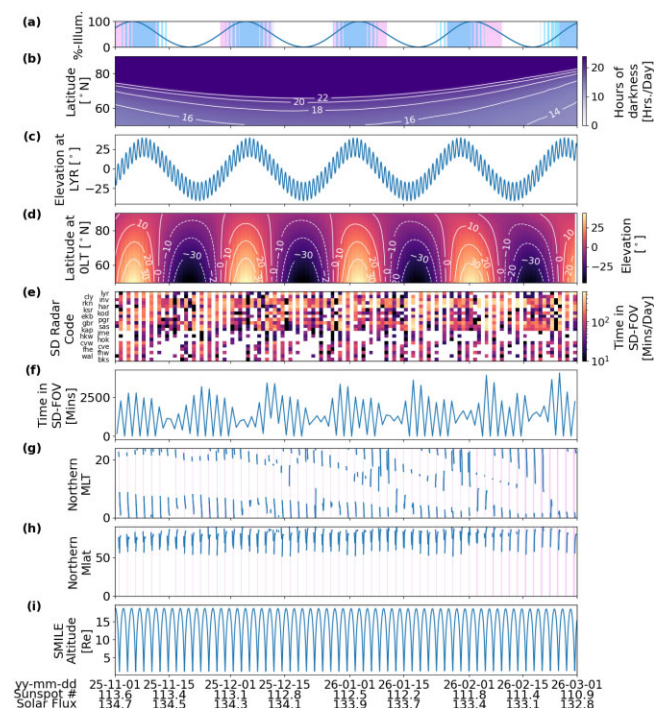
Figure 1. Multipanel plot showing (from top to bottom): (a) per cent of the moon illuminated by the Sun, assuming the face of the moon is a circular disc [times where the solar illumination of the moon is greater than 50 per cent are shaded lighter (in pink), darker colour (blue shade) shows when the elevation of the moon at Longyearbyen (LYR) is greater than 10°]; (b) Number of hours of darkness per day for latitudes north of 50°N; (c) the elevation of the moon at Longyearbyen (situated at 78.2°N latitude); (d) the elevation of the moon at midnight for latitudes north of 50°; (e) coverage of SMILE footprint by SuperDARN radars; (f) total SuperDARN Coverage; (g) MLT of the SMILE footprint; (h) northern magnetic latitude of the SMILE Footprint and (i) SMILE Altitude.

tools, which we use to plan for conjunctive observing campaigns. Whilst the SMILE orbits may not be final, these plots give us an indication of what we will expect and can be updated for future campaigns.

The nine time series presented in Fig. 1 serves as a guide on the favourable conditions and likely impacts for the first SMILE Northern hemisphere winter (2025 November until 2026 March). These figures are made with data extracted from the Data Fusion Facility (DFF) (https://www.smile-fusion.le.ac.uk/) (Carter et al. 2024), which is purpose-built to facilitate ground-based and additional science with SMILE. An important part of these studies will come from night observations of auroral activity from ground based ASIs. Unfortunately, data from ASIs will become compromised in the presence of light-pollution from a sun-lit moon. Providing a measure for the amount of moonlight at the footpoint of the SMILE ephemeris is a non-trivial task (see Patat 2004) and is beyond the scope of this paper. Therefore, we use Fig. 1(a) to (d) to help assess periods most affected by light pollution from the moon on ASIs. Fig. 1(a) shows the per cent of the moon illuminated by the Sun, assuming the face of the moon as a circular disc. An illumination of 100 per cent corresponds to a full moon (for more information see definitions listed on https://ssd.jpl.nasa.gov/horizons/manual.html). Periods of high light pollution are found when the elevation of the moon above the horizon at Longyearbyen (situated at 78.2°N latitude) is greater than 10° and approaching the full moon phase

Table 1. Model inputs for Fig. 1.

Code input variables (units)	Input value
model	'T96'
sym (nT)	100.0
by (nT)	0.0
bz (nT)	0.5
vx (km s^{-1})	300.0
vy (km s^{-1})	0.0
vz (km s^{-1})	0.0
n_p (cm^{-3})	0.5
$pdyn$ (nPa)	$\frac{(n_p*(100.0^3)*((vx*1.0e^{03})^2)*m_p)}{1.0e^{-9}}$
$altitude$ (km)	100.0

[which we have arbitrarily assigned with the solar illumination of the moon being greater than 50 per cent, as shown in panel Fig. 1(a) by regions shaded in pink or co-shaded in pink/sky-blue]. Overall, the shaded regions where the moon's illumination is high is particularly unfavourable for auroral observations, so this allows us to quickly distinguish which periods are of interest. The following panels show: (b) the hours of darkness per day for latitudes north of 50°N; (c) the elevation of the moon at Longyearbyen (LYR), which is a great location for ground-based optical observations of the cusp aurora during Arctic winter; (d) the elevation of the moon at midnight for latitudes north of 50°N; (e) the maximum possible coverage of the SMILE footprint by SuperDARN radar; (f) the total possible SuperDARN coverage of the SMILE footprint; (g) the field line trace values of the SMILE footprint in northern magnetic local time (MLT); (h) and the northern magnetic latitude (MLAT) of the field-line tracing. The SMILE ephemeris were evaluated for an expanded magnetosphere using the Tsyganenko 96 model (Tsyganenko & Stern 1996) in PyGeopack (James 2023). From this the footprint locations in MLT and MLAT were extracted. Despite employing the expanded magnetosphere conditions detailed in Table 1, modelling challenges remain. This is evidenced by data gaps in the MLT and MLAT (panels g and h), attributed to difficulties in field line tracing from high-altitude positions in the cusp/polar region. In these cases, deviations in field line tracing can exceed limits set within the Geopack field line tracing algorithms to ensure a reliable tracing. Finally, panel Fig. 1 (i) shows the SMILE altitude. We have used the current ephemeris available and these are for illustrative purposes only. Whilst the ephemeris are still likely to change, the expected changes to the planned orbits are small. Furthermore, by producing this work now, we have infrastructure ready to go to be able to adapt once the final ephemeris becomes available post launch.

Fig. 2 shows a zoomed-in version of Fig. 1 from 2025 mid-December to 2026 mid-January. From the first panel we see that around half the time period shown will be illuminated by the moon, so it is unfavourable for auroral observations from the ground (pink region and blue). As shown by panel (c), this coincides when Longyearbyen is more illuminated by the moon. From panels (e) and (f), which show the SuperDARN coverage of the SMILE footprint, we see that there are a number of intervals which could be favourable for conjunction observations with SMILE. Based on the moonlight illumination and SuperDARN coverage, the 16th and 18th December, as well as 10th-15th January present excellent dates for observing. The 2025 December 21st–24th period where both SuperDARN and ground auroral observations in theory should be possible, are unfortunately unfavourable as this falls on the Christmas holiday period where many facilities are either inaccessible or not crewed/operational (e.g. EISCAT facilities, Kjell Henriksen Observatory, etc.).
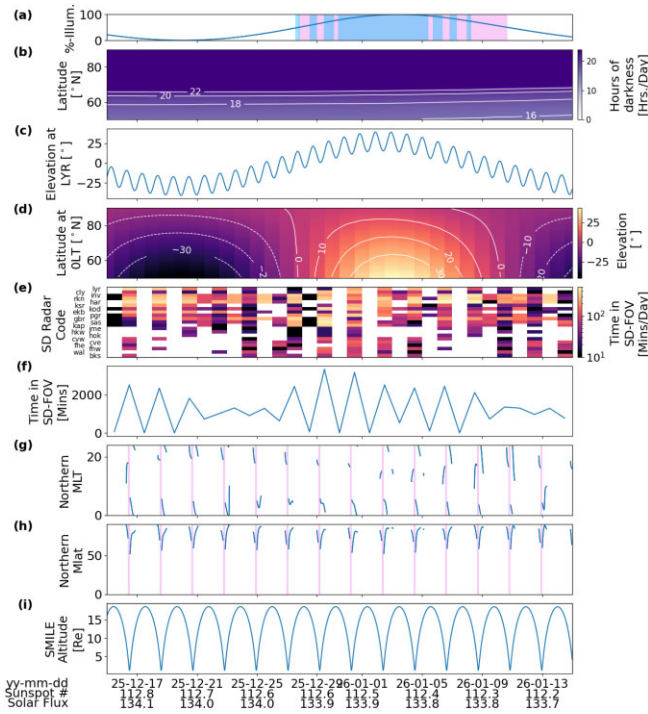
Figure 2. Multipanel plot showing the same panels as Fig. 1. The time series is zoomed in, showing one month from 2025 mid-December until 2026 mid-January.
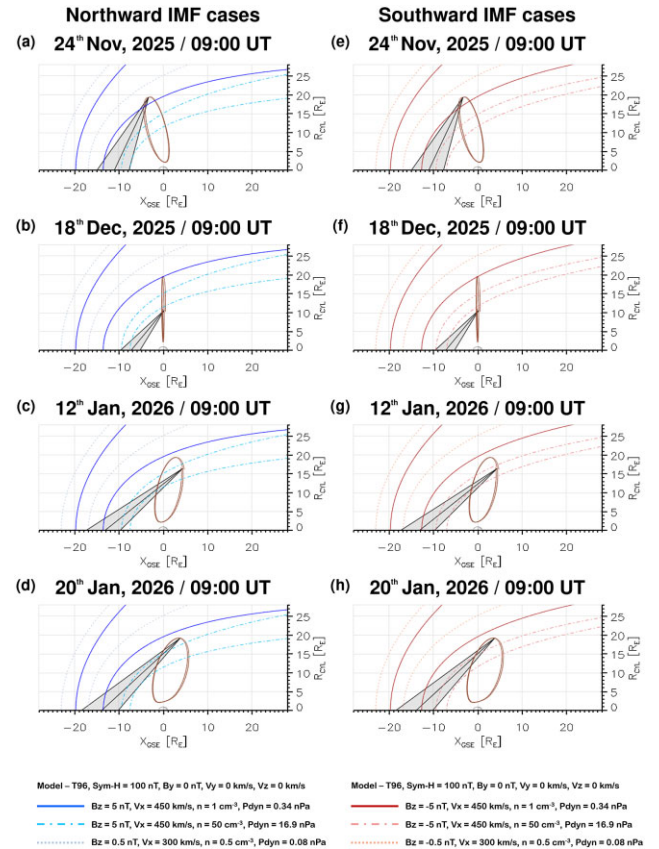

Figure 3. Multipanel figure showing four example conjunctions from 2025 November 24th (a and e), 2025 December 18th (b and f), 2026 January 12th (c and g), and 2026 January 20th (d and h). Each panel shows a side-view of the SMILE orbits as it slices the magnetosheath for different possible solar wind conditions, modelled using Geopack with the T96 model (Tsyganenko & Stern 1996). Areas shaded in grey present the configuration of the SMILE SXI field of view for the respective date and time of each panel. The left column shows examples of different northward IMF cases and the right column shows examples of southward IMF cases. Different shades of colour and line-styles display the bow shock and magnetopause locations using the different solar wind conditions, the details of which are listed below the bottom panels of the figure.

Fig. 3 shows the SMILE orbit ± 52 h of different conjunction times and potential solar wind conditions. The SMILE orbit plots use Geocentric solar ecliptic (GSE) coordinates in a cylindrical representation, where the vertical axis shows the radial extent of the Y_{GSE} and Z_{GSE} coordinates ($[Y_{GSE}^2 + Z_{GSE}^2]^{1/2}$). It should be noted that the apoapsis of the SMILE orbit occurs over the Northern hemisphere and conversely the periapsis occurs over the Southern hemisphere. The Chao et al. (2002) and Shue et al. (1997) models are used to find the locations of the bow shock (most distant from the origin) and magnetopause, respectively, and are plotted in pairs of the same shade of colour and line-style. Different shades of colour and line-styles display the bow shock and magnetopause locations using the different solar wind conditions, the details of which are listed below the bottom panels of the figure. The rows show a different date each: 2025 November 24th (first row), 2025 December 18th (second row), 2026 January 12th (third row), and 2026 January 20th (last row), and the two columns show northward (left) and southward (right) cases each. We see that according to the Tsyganenko model (Tsyganenko & Stern 1996), the SMILE orbits will slice into the magnetosheath for almost all cases, except for the extended magnetosphere case using low solar wind pressure (Pdyn = 0.08 nPa) and low solar wind magnetic field (IMF $B_Z = \pm 0.5$ nT). At a solar wind pressure of 0.34 nPa (and IMF $B_Z = 5$ nT), SMILE will encounter the magnetopause during November only. At a solar wind pressure of 16.9 nPa (and IMF $B_Z = 5$ nT), the SMILE orbit will traverse the magnetosheath entirely. We predict that the spacecraft will cross the magnetosheath twice. Our solar wind conditions are showing extreme cases in comparison to the solar wind conditions over the last solar cycle: OMNI data from the last solar cycle shows that the solar wind dynamic pressure is $<=0.08$nPa 0.06 per cent of the solar cycle, $<=0.34$nPa 0.8 per cent of time, $>=3.4$nPa 11 per cent of time, and $|B_z| >=5$nT 10 per

cent of time (in both tails). This means that whilst B_z is close to the average for our most extended case, the unusually low solar wind pressure ($Pdyn = 0.08$ nPa) makes it an infrequent case. The case for the most contracted magnetosphere ($Pdyn=16.9$ nPa) is the more likely case to occur according to data from the last solar cycle. This case has the strongest driving and is more favourable for imaging the subsolar magnetopause, whereas the two weaker driving conditions (and less likely to occur, according to the last solar cycle) would require very long integration times for sufficient photon counts. Conversely, weaker driving conditions better for in situ observations of cusp if the orbit allows observations. For studies where in situ data from the magnetosheath is required, we therefore recommend planning for 2025 November, as this is when the spacecraft is most likely to find itself in this region, for a variety of solar wind pressures. Similarly, in situ measurements of the high-latitude magnetopause's motion appear to be more likely for the 2026 January case when the apogee, where the spacecraft dwells the longest during each orbit, is closer to all the model boundaries. The presented SMILE orbits are preliminary, so whilst our recommendations hold for the currently planned orbital configurations, these may change. The figures and
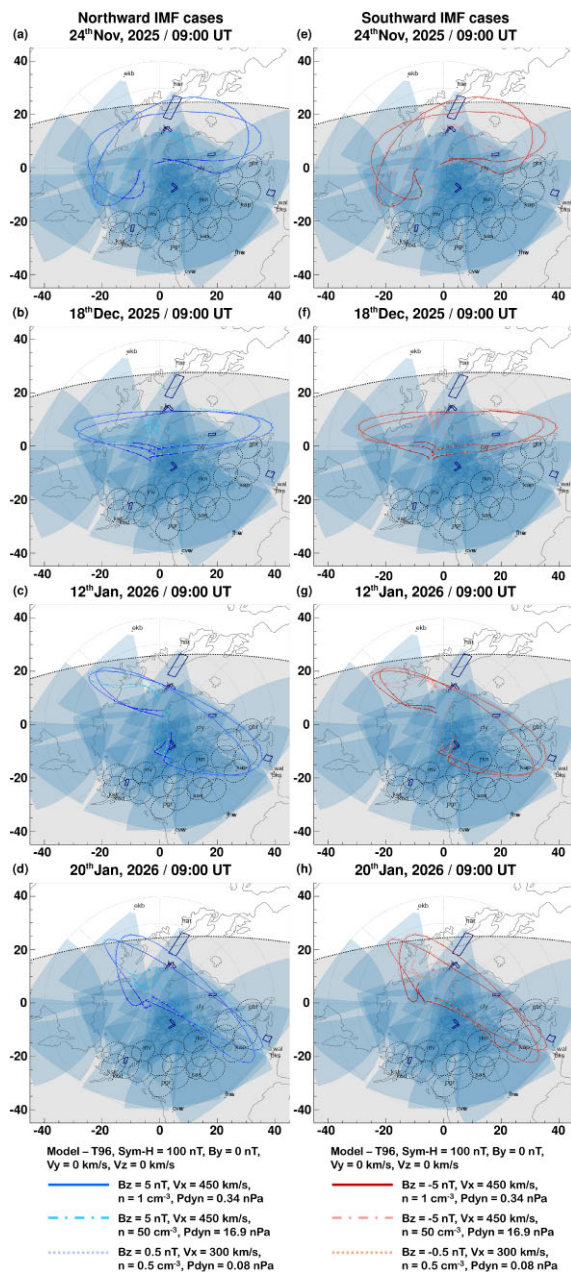
Figure 4. Multipanel figure showing a view on the ground for the same example conjunctions as in Fig. 3. Shaded fan-shaped areas show the SuperDARN radar fields of view, the dashed circles show the ground-based all-sky imagers, and the fields of view of incoherent scatter radars are shown by the dark rectangles. The black dotted line shows the day-night terminator. The columns shows traces of the SMILE orbit footprints for the same cases as in Fig. 3 for northward (left column) and southward (right column) IMF cases.

analysis of possible observations does however highlight possibilities and how existing tools may be used in planning for future campaigns.

Fig. 4 shows the same time periods and orbits as in Fig. 3, but from a perspective of ground coverage. Each panel shows the SuperDARN fields of view and other ground-based instrumentation, such as the all-sky imager chain across Canada. The same solar wind conditions as were shown in Fig. 3 are used to trace the SMILE footprint to the ground along magnetic field lines using the GEOPACK software (James 2023). We see immediately that there is little difference between the solar wind conditions and where the model locates the footprint of

SMILE. We also see that whether or not the IMF is northward or southward makes little difference, unless the spacecraft finds itself in the magnetosheath. What is however striking about these different cases is that the orbital geometry severely affects coverage from ground-based instrumentation. All cases show good overlap with the SuperDARN field of views, and due to the time of day, all cases see the SMILE footprint potentially traversing the area around Svalbard where auroral cameras are available. The January cases show SMILE not only passing by Svalbard, they also all show good coverage with the north American all-sky imager chain. The November cases show SMILE passing over northern Fennoscandia where EISCAT_3D and a variety of auroral instruments are located observing a wide range of spatial scales.

It is clear from Figs 1 to 4 that not all types of conjugate observations with SMILE and ground based instrumentation will be possible at all times. To ensure that we benefit maximally from the opportunities of SMILE's first Northern hemisphere winter, we have chosen several science themes for the Winter Campaign with each theme utilizing different instrumentation and focusing on a different aspect of observations. The themes for the SMILE Winter Campaign are:

(i) Earth's magnetosheath, magnetopause, and magnetic cusp impact on the ionospheric cusp region;
(ii) Defining the relationship between auroral processes, solar wind, and magnetospheric drivers;
(iii) Understanding the interhemispheric properties of the Earth's magnetosphere-ionosphere system.

We will discuss each one of these and how it can be achieved in the following sections.

3.1 Earth's magnetosheath, magnetopause, and magnetic cusp impact on the ionospheric cusp region

SMILE will be the first mission in polar orbit to observe the X-ray emission from charge exchange of high charge state solar wind ions and exospheric neutrals in the magnetosheath and cusp (Branduardi-Raymont et al. 2018; Branduardi-Raymont & Wang 2022). By applying fits to observed 2D X-Ray photon counts from SMILE, the Northern hemisphere cusp location may be identified as a bright spot at times when the observational angle is favourable and charge exchange is high (Jorgensen et al. 2019). New techniques for a successful fitting to the modelled X-Ray photon counts from SMILE are explored for a substorm interval, Carter et al. (private correspondence). Existing mapping techniques, as was used for Figs 1 and 4, allow an estimated location of the cusp to be traced to the ionosphere. Using ground-based, high latitude optical observations of the dayside aurora, in particular in the red line at 630 nm and green line at 557.7 nm (e.g. from auroral imagers and meridian scanning photometers located at the Kjell Henriksen Observatory, Svalbard), we will be able to observe cusp aurora at the location determined from SMILE observations. Of particular interest are poleward moving auroral forms (PMAFs) (Fasel 1995; Oksavik, Moen & Carlson 2004; Sandholt, Farrugia & Denig 2004; Fear et al. 2017), which are thought to be a signature of flux transfer events (FTEs) and direct-entry solar wind plasma following dayside reconnection, and polar cap patches which are regions of enhanced ionospheric density transported across the polar cap from the dayside cusp region (Weber et al. 1984; Lockwood & Carlson 1992; Carlson et al. 2004). Being able to observe these in context will allow novel insights, which will address the top level science question of SMILE '*What are the fundamental modes of the dayside solar wind/magnetosphere interaction?*' (Branduardi-Raymont & Wang 2022). Observations of

the cusp aurora, which coincide with mapped cusp locations will enable to answer open science questions, such as:

● *How quickly are changes at the magnetopause reflected in the auroral footprint (e.g. investigate auroral signatures of cusp reconnection or modulation by ULF waves)?* We propose to explore the mechanism of communication between the magnetopause and ionosphere and its associated time-scale for different physical solar wind–magnetosphere coupling processes such as cusp reconnection or ULF wave boundary dynamics. Linking the magnetopause to aurora is very difficult as thus far, we have only had serendipitous magnetopause crossings with the current suite of in situ spacecraft e.g. MMS. With SMILE we will have almost continuous measurements of the magnetopause boundary and the cusp. By imaging the cusp with SXI, we can determine cusp location and infer cusp structure and its time evolution in space. This may then be related to ground-based observations using the DFF and their meridional structure to understand the coupling from the cusp to the ionosphere, mapping of which is poorly understood.

● *Why are PMAFs so strongly correlated with IMF By dominated conditions (e.g. Sandholt et al. 2004), and throat aurora so strongly correlated with IMF Bx dominated conditions (e.g. Han et al. 2019)?* PMAFs will be tracked using UVI, which will provide instantaneous imaging of large areas of the aurora, providing a clear benefit over current space-based auroral imaging capabilities, which only image swaths at a cadence of ∼25 min (DMSP/SSUSI).

● *What is the meridional structuring of (particularly transient ULF wave) dynamics in the vicinity of the cusps and where do they map out into space (e.g. Pilipenko et al. 2015; Kozyreva et al. 2019).* Similar to the point above, measuring dynamics within the magnetic cusp in situ is very difficult. SMILE SXI will provide an unparalleled opportunity to remote sense the cusp, which alongside measurements on the ground and in the ionosphere may solve current mapping ambiguities of the meridional structures observed in the cusp-region on the ground.

Being able to observe the cusp location in situ using the light ion analyser, alongside ground-based observatories will allow us to place the cusp into a wider context. To trace when the LIA is on a field line will be achieved using the the DFF and spacecraft modelling, using the tools under development for conjunction planning and shown in the figures. The in situ observations will be dependent on solar wind conditions, as shown by the orbits in Fig. 3. Crucial to this wider context is the plasma convection of the magnetosphere: The magnetosphere responds to solar wind driving via reconnection (e.g. Milan et al. 2017; Walach et al. 2017; Fuselier et al. 2024) and boundary motion (e.g. Archer et al. 2024), both of which drive plasma around the magnetosphere. This is known as plasma convection and it can, thanks to the field-aligned currents coupling magnetospheric convection to the ionosphere, be measured from the ground using radar systems such as SuperDARN (e.g. Chisham et al. 2007). Measuring the convection with SuperDARN, as well as simultaneous to the SMILE-derived traced cusp location will allow us to further investigate plasma flows and how this changes across different solar wind drivers and cusp locations. This will be facilitated by the DFF. It will allow us to address the open questions:

● *How quickly are changes in the magnetopause location reflected in the convection pattern?* Studying changes in the magnetopause location and how they are reflected in the convection pattern is inherently difficult and SMILE will provide a new opportunity. Furthermore, this will help us to answer a big outstanding prob-

lem: Accurate magnetic field mapping between the ionosphere and magnetosphere, especially during geomagnetically active times (Borovsky et al. 2020). Remote and in situ observations of the cusp alongside ionospheric/ground measurements will enable testing the conjugacy of current mapping techniques and the time-scales on which changes are mirrored in the ionosphere.

● *What transient and quasi-static changes in the convection patterns occur when the magnetopause location shifts?* Observing transients is inherently difficult and SMILE will provide an unprecedented opportunity to study this, as outlined by Branduardi-Raymont & Wang (2022) and Branduardi-Raymont et al. (2018).

3.2 Defining the relationship between auroral processes, solar wind, and magnetospheric drivers

The last time that large-scale, high-cadence observations of the entire auroral oval were captured with spacecraft such as the IMAGE or Polar missions, fewer ground-based instruments were available. This makes the Winter Campaign time period especially interesting for observing the auroral oval alongside other ground based instrumentation. To better understand top level SMILE science question 1 ('*What are the fundamental modes of the dayside solar wind/magnetosphere interaction?*'), we will map the auroral oval location alongside auroral images from the ground (e.g. SMILE ASI and auroral imagers and meridian scanning photometers located at the Kjell Henriksen Observatory, Svalbard). If the auroral oval location overlaps with the EISCAT_3D field of view, we will also be able to observe multispatial, 3D structures in the aurora, using EISCAT_3D, which will add further values. This will allow us to answer:

● *Are FUV auroral emissions always co-located with visible aurora and vice versa?* Auroral emission, especially on the dayside is complex and dynamic (e.g. Hu et al. 2009; Hosokawa et al. 2020) and questions remain. For example, how electromagnetic energy is converted to particle energy in the aurora remains a gap in our understanding (e.g. Borovsky et al. 2020, and references within). Understanding the links between the more energetic FUV aurora, and the visible aurora, which is less energetic, will build a better understanding of auroral emission.

● *How do auroral boundaries at different scales respond to solar wind transients?* The SMILE UVI instrument will have a spatial resolution of ∼100 km and a 10° circular field of view, whereas ground-based instrumentation can achieve much higher resolution. Linking these observations will allow testing of how solar wind transients affect different scale-sizes and the aurora, including waves along the auroral boundaries, which may be linked to Kelvin-Helmholtz instabilities at the magnetopause. For example, we will be able to verify hypotheses and models such as the one set out by e.g. Johnson et al. (2021).

● *What is the role of polar cap arcs, streamers, and optical transients and their dependencies on quasi-static auroral structures?* Polar cap arcs, streamers, and optical transients have been linked to magnetospheric phenomena such as substorms on many occasions and thus play crucial roles in the dynamic interactions within the Earth's magnetosphere and ionosphere, each with specific dependencies on quasi-static auroral structures and broader solar wind and magnetospheric conditions. Understanding these dependencies helps in comprehending the overall behaviour of the auroral phenomena and their impact on the magnetospheric dynamics. SMILE will

provide a unique opportunity to monitor these alongside ground-based observations.

Furthermore, we aim to trace SuperDARN convection patterns across the auroral images. With the addition of search coil magnetometers, we will also be able to identify substorm-related ULF waves that are useful in monitoring the development of substorms. We propose the use of search coil magnetometers from existing ground based arrays such as MICA as an example: The sampling rate of the MICA search coils can be either 10 Hz or 20 Hz depending on specific installation, providing a Nyquist frequency (an effective limit of frequencies that can be probed with this instrumentation) of either 5 Hz or 10 Hz. Additionally, the frequency response of the MICA search coil system peaks at around 2.5 Hz. Therefore the MICA search coils are keyed to study ULF waves in the PC 1–2 bands between 0.1 and 5 Hz, such as EMIC or ECH waves (Engebretson et al. 2009; Kim 2010; Salzano et al. 2022). These search coil magnetometers, which are sensitive to magnetic field time variations, nicely complement fluxgate magnetometers that typically sample at ~ 1 Hz and measure DC and lower frequency variations related to quasi-static currents and Pc3-5 ULF waves.

This will allow us to delve deeper into SMILE top level science questions 2 and 3 ('*What defines the substorm cycle?*' and '*How do Coronal Mass Ejection (CME)-driven storms arise and what is their relationship to substorms?*'). The convection captures the bulk plasma transport in the ionosphere–magnetosphere system, whilst the auroral emission captures the acceleration of particles and loss mechanisms. EISCAT_3D will provide further detail on a smaller scale, which will allow us to explore the multiscale nature of magnetosphere–ionosphere electrodynamics and the aurora. Examining these data in tandem, especially during substorms and geomagnetic storms, will allow us to answer:

● *Can the substorm phenomena be considered separate from the convection (or Dungey) cycle?* Ongoing controversies exist with respect to the onset and triggering of substorms and the respective roles of auroral streamers, Alfvén waves, and auroral beads (see discussion in Carter et al. 2024). With SMILE's new auroral observations, we will be able to observe auroral substorms as they unfold, including potential triggers and preliminary phenomena (like streamers or beads) whilst also observing the convection with SuperDARN at unprecedented detail. Surveying sporadic phenomena, such as substorms, will allow us to infer how they are linked to global magnetospheric dynamics, such as convection.

● *Are the convection and auroral emission different during geomagnetic storm-time substorms versus non-storm-time substorms?* During geomagnetic storm times, the magnetosphere changes drastically, which affects a number of dynamic processes. For example, ULF-wave power enhancements (Sandhu et al. 2021), electron loss and enhancements in the outer radiation belt (Walton et al. 2022), pitch-angle scattering of electrons in the closed magnetosphere (Walton et al. 2023), alongside changes in the convection region in the ionosphere are all affected (Walach & Grocott 2019; Walach, Grocott & Milan 2021). Changes, such as the addition of a plasmaspheric plume add to a complicated set of dynamics, which are not yet fully understood (Sandhu et al. 2023). For example, the outflow from a plasmaspheric plume during geomagnetic storms may quench or slow down dayside reconnection (Borovsky et al. 2020), which in turn will affect convection and potentially auroral emission. The last decade of observations has been relatively quiet with few large geomagnetic storms. We are expecting the next few years to include more extreme geomagnetic storms, which will allow novel

observations to be captured. By combining the new SMILE data sets with ground-based data, we will discern boundary changes of the convective and auroral region and link these to plasmasperic boundary changes from SMILE measurements, which will allow us to discern these dynamics further.

3.3 Understanding the interhemispheric properties of the Earth's magnetosphere–ionosphere system

The magnetosphere–ionosphere current systems and many waves are inherently asymmetric in a north–south and/or an east–west sense. For example, dayside transients such as interplanetary shocks, ion foreshock transients, or magnetosheath jets often exert dynamic pressure on the magnetopause asymmetrically with respect to the Earth–Sun line. The same is true on the nightside for a wide range of transients. These asymmetries in turn dictate the types of current systems/waves that are generated (e.g. Oliveira et al. 2020). UVI imaging from SMILE will enable us to pinpoint the location of auroral intensifications related to asymmetric disturbances, while networks of ground-based magnetometers and ASI, as well as global SuperDARN flow patterns, will reveal the asymmetric 2D disturbances in ionospheric currents and waves. For example, observations from pairs of conjugate points in the two hemispheres can be used to determine the mode of magnetic oscillations and associated asymmetry (e.g. Sugiura & Wilson 1964). Furthermore, SMILE will measure in situ plasma dynamics with the magnetometer (MAG) and the light ion analyser (LIA). These direct measurements of perturbations and mesoscale structures in the plasma and magnetic field will accompany ground-based measurements. Using field-line tracing, the in situ measurements can be traced to ground-based observations and reveal multidimensional information of asymmetries and electrodynamics. Expanded networks of ground-based observations in both hemispheres (Arctic and Antarctic), combined with SMILE remote sensing of the cusp/auroral oval in the Northern hemisphere, will enable novel investigations of asymmetries related to mesoscale 2D structures that advance previous work in this area using more sparse observations (e.g. Murr et al. 2002). This, in turn, will reveal how asymmetric drivers on the dayside/nightside ultimately affect magnetosphere–ionosphere coupling processes. It will allow us to answer:

● *How do asymmetric drivers on the day/nightside affect magnetosphere/ionosphere coupling and propagate through the system?* SMILE will image dawn/dusk asymmetric compression of the magnetosphere in response to solar transients, such as interplanetary shocks. Combining imaging (both SXI-derived and UVI) with in situ LIA and MAG measurements and ground based magnetometer measurements, SuperDARN and ASI will be a powerful combination. By studying these data sets in conjunction, we will be able to answer the long-standing question: Are asymmetries in ground response to interplanetary shocks due to shock impact angle causing asymmetric compression of the magnetosphere? This interpretation has not been directly demonstrated as one cannot easily monitor the magnetopause at different local times with in situ spacecraft (Oliveira 2023). SMILE may be able to image (dawn/dusk) asymmetric compression of the magnetosphere during strong driving, resolving this question.

Depending on the orbital geometry used, addressing this theme links to all three of the top level SMILE science questions: '*What are the fundamental modes of the dayside solar wind/magnetosphere interaction?*', '*What defines the substorm cycle?*' and '*How do Coronal Mass Ejection (CME)-driven storms arise and what is their relationship to substorms?*'(Branduardi-Raymont & Wang 2022).

4 CAVEATS

For dayside auroral or cusp science, there will be a need to map the cusp to the ground. This will be dependent on the viewing geometry of SMILE and sufficient signal to noise in the SXI images to allow for boundaries to be determined at an acceptable cadence to probe the science question of interest. Furthermore, reconstruction of 3D real space from 2D line-of-sight integrated images is tricky and often requires an assumed shape, as explained in methods being developed for the magnetopause but equivalently relevant to the cusps (Wang & Sun 2022). Specifically for the cusp, mapping meridional structuring of the cusp out in space require assumptions of symmetry about some assumed cusp axis orientation. For all science requiring SuperDARN and auroral imager data, there is also a dependence on atmospheric conditions: Any ground-based imagers will need a dark, cloud-free night with minimal moonlight. SuperDARN radars can be switched on to the correct operating mode, but in order to make observations, they require ionospheric field-aligned irregularities to produce backscatter (e.g. Chisham et al. 2007), which cannot be controlled. For the science in Section 3 on asymmetries, there is an orbital dependence: the field line tracing to the magnetometer locations has to work in both hemispheres.

4.1 Accessing EISCAT_3D data

Another possibility is that SMILE is included in the EISCAT All Associate time. This is a pool of time that is donated by the Associates to support modes beneficial to all, usually revolving around satellite conjunctions. In the past, this has been used to support Cluster operations and more recently SWARM and ARASE measurements. Using a combination of these access pathways, alongside traditional associate time from EISCAT member countries, EISCAT_3D has an exciting potential to support SMILE in the Winter campaign. The funding model for EISCAT causes some restrictions on the use of data: current associates (China, UK, Norway, Sweden, Finland, Japan) are entitled to embargo their data for a year after an observation is made on their behalf. This can be waived for collaborations. However, any scientist can gain access to time on the radars via two principle routes: the EISCAT peer review programme and the World Day Programme. The Peer review programme is hosted by EISCAT such that any scientist can apply for time with a strong science case. In the World Day Programme proposals are targeted at specific science goals that are best supported by multiple radars operating simultaneously. This has the advantage of ensuring that measurements are made, not just by EISCAT, but by other Incoherent Scatter Radars (ISR) such as the Resolute Bay Incoherent Scatter Radar (RISR) systems and Millstone Hill for a coordinated period of around 5 d.

4.2 Observational challenges

These caveats provide significant challenges. Observational difficulties which are out of the control of the observer, such as poor coverage or cloudy nights, can hinder scientific studies. The best mitigation technique for these issues is being prepared and planning early to maximize the number of hours where ground-based data are available: When we aim for the first possible observation window and face challenges which are out of our control, we may have a chance to try again, so it is prudent to plan ahead to leverage the most science. Furthermore, some ground-based instruments, such as the SuperDARN radars operate on a schedule and operating modes can be requested with approximately two months warning.

SuperDARN mostly operates a common time mode, which works well for producing convection maps (e.g. Thomas & Shepherd 2018), but any other modes (e.g. frequency sweeps or stationary camping beams) have to be specifically requested. Other facilities, such as EISCAT_3D may require longer observation planning periods, but if overcome, can yield great scientific returns. Thus, planning ahead is crucial to ensuring the correct information is captured.

5 SUMMARY

The SMILE mission provides a unique opportunity to observe the coupling in the Earth's magnetosphere–ionosphere system. SMILE will provide novel and unprecedented measurements of the plasma dynamics which drive elusive magnetospheric activity, such as geomagnetic storms and substorms. The SXI instrument, for example, will image the X-ray charge exchange emission from the magnetospheric cusp for the first time. The UVI auroral imager will allow us to see the entire auroral oval for the first time since the IMAGE spacecraft lost contact in 2005. The launch of SMILE provides an exciting opportunity: For the first time, we will be able to combine these measurements with an unprecedented wide suite of ground-based observatories. SuperDARN, for example, has expanded geographically, but also in its capability with new digital radars allowing for high-cadence imaging of the ionosphere. Leveraging existing ground-based infrastructure in a coordinated way will allow us to answer new science questions in addition to the SMILE science goals. This white paper has summarized these additional science goals surrounding the first Northern hemisphere winter of SMILE operations. The aim is to provide contextual and extra science observations, which will advance the overarching mission goals of SMILE and maximize the scientific return. This white paper does not capture all possible scientific advances, but outlines some science gaps which we will be able to fill. We thus call the scientific community to action to plan for this exciting time and use this white paper as a resource for planning to enable novel scientific return.

DATA AVAILABILITY

Ephemeris data of the Moon used in Panel (a) of Figs 1 and 2 can be found via NASA's Horizons on-line solar system data (https://ssd.jpl.nasa.gov/horizons/app.html/).

Panels (c) and (d) of Figs 1 and 2, were created using ephemeris data of the Moon and specific coordinates on the Earth, as calculated with the SPICEYPY python wrapper (https://doi.org/10.21105/joss.02050) for the NASA's Navigation and Ancillary Information Facility (NAIF) SPICE Toolkit (https://naif.jpl.nasa.gov/naif/).

Values of predicted sunspot number and solar flux units used in the x-axis labels of Figs 1 and 2 can be found via NOAA's Space weather and prediction center, https://www.swpc.noaa.gov/products/solar-cycle-progression.

Panels (e) to (i) of Figs 1 and 2, and plots of Figs 3 and 4 were created using data from a local version of the publicly available SMILE DFF, where similar plots to those in the paper may be created by a user. Due to the extended time periods used in this study, slight modifications to the public code were required. These are available on request. Tracing of magnetic field lines within the SMILE DFF are achieved using the PYGEOPACK python wrapper for Geopack-2008 (https://pypi.org/project/PyGeopack/).

The SMILE DFF and other plots in this paper rely on solar wind and geomagnetic activity data provided by OMNI found via https://omniweb.gsfc.nasa.gov/.

ACKNOWLEDGEMENTS

REFERENCES

Archer M. O., Shi X., Walach M.-T., hartinger M. D., Gillies D. M., Di Matteo S., Staples F., Nykyri K. 2024, Front. Astron. Space Phys., 11, 1430099

Borovsky J. E. et al., 2020, J. Atmos. Sol. Terr. Phys., 208, 105377

Branduardi-Raymont G., Wang C., 2022, Bambi C., Santangelo A., eds, SMILE: A Novel Way to Explore Solar-Terrestrial Interactions. Springer Nature, Singapore, p. 1

Branduardi-Raymont G. et al., 2018, Smile Definition Study Report (Red Book). European Space Agency, ESA/SCI, Nordwijk, the Netherlands

Carlson H. C., Jr, Oksavik K., Moen J., Pedersen T., 2004, Geophys. Res. Lett., 31, L08806

Carter J. A. et al., 2024, Earth Planet. Phys., 8, 275

Chao J. K., Wu D. J., Lin C. H., Yang Y. H., Wang X. Y., Kessel M., Chen S. H., Lepping R. P., 2002, in Lyu L.-H., ed., Space Weather Study Using Multipoint Techniques, Cospar Colloquia Ser. Vol. 12. Elsevier, Oxford, p. 127

Chisham G. et al., 2007, Surv. Geophys., 28, 33

Cravens T. E., 1997, Geophys. Res. Lett., 24, 105

Engebretson M. J., Moen J., Posch J. L., Lu F., Lessard M. R., Kim H., Lorentzen D. A., 2009, J. Geophys. Res.: Space Physics, 114, A06217

Fasel G. J., 1995, J. Geophys. Res.: Space Phys., 100, 11891

Fear R. C., Trenchi L., Coxon J. C., Milan S. E., 2017, J. Geophys. Res.: Space Phys., 122, 12310

Fuselier S. A. et al., 2024, Space Sci. Rev., 220, 34

Han D.-S. et al., 2019, Geophys. Res. Lett., 46, 7113

Hosokawa K., Kullen A., Milan S., Reidy J., Zou Y., Frey H. U., Maggiolo R., Fear R. 2020, Space Sci. Rev., 216, 15

Hu Z.-J. et al., 2009, J. Atmos. Sol. Terr. Phys., 71, 794

Huyghebaert D. et al., 2024, EGUsphere, 2024, 1

James M. K. 2023, PyGeopack, Zenodo, available at: https://zenodo.org/records/8133033

Johnson J. R., Wing S., Delamere P., Petrinec S., Kavosi S., 2021, J. Geophys. Res.: Space Phys., 126, e28583

Jorgensen A. M., Sun T., Wang C., Dai L., Sembay S., Wei F., Guo Y., Xu R., 2019, J. Geophys. Res.: Space Phys., 124, 4365

Kim H. 2010, Development of Ground-based Search-Coil Magnetometer Systems in the Polar Regions and Studies of ULF Pc 1–2 Wave Propagation in the Ionospheric Waveguide. University of New Hampshire, Durham

Kozyreva O., Pilipenko V., Lorentzen D., Baddeley L., Hartinger M., 2019, J. Geophys. Res.: Space Phys., 124, 9058

Lockwood M., Carlson H. C., Jr, 1992, Geophys. Res. Lett., 19, 1731

McWilliams K. A., Detwiller M., Kotyk K., Krieger K., Rohel R., Billett D. D., Huyghebaert D., Ponomarenko P., 2023, Radio Sci., 58, e2022RS007591

Milan S. E. et al., 2017, Space Sci. Rev., 206, 547

Murr D. L., Hughes W. J., Rodger A. S., Zesta E., Frey H. U., Weatherwax A. T., 2002, J. Geophys. Res.: Space Phys., 107, SIA14–1

Nishitani N. et al., 2019, Prog. Earth Planet. Sci., 6, 27

Oksavik K., Moen J., Carlson H. C., 2004, Geophys. Res. Lett., 31, L11807

Oliveira D. M. 2023, Front. Astron. Space Sci., 10, 1179279

Oliveira D. M., Hartinger M. D., Xu Z., Zesta E., Pilipenko V. A., Giles B. L., Silveira M. V. D., 2020, Geophys. Res. Lett., 47, e90857

Owens M. J., Lockwood M., Barnard L. A., Scott C. J., Haines C., Macneil A. 2021, Sol. Phys., 296, 82

Patat F. 2004, The Messenger, 118, 11

Pilipenko V., Belakhovsky V., Engebretson M. J., Kozlovsky A., Yeoman T. 2015, Ann. Geophys., 33, 395

Salzano M. et al., 2022, J. Geophys. Res.: Space Phys., 127, e2022JA030600

Sandholt P. E., Farrugia C. J., Denig W. F. 2004, Ann. Geophys., 22, 613

Sandhu J. K., Rae I. J., Staples F. A., Hartley D. P., Walach M.-T., Elsden T., Murphy K. R., 2021, J. Geophys. Res.: Space Phys., 126, e29337

Sandhu J. K., Degeling A. W., Elsden T., Murphy K. R., Rae I. J., Wright A. N., Hartley D. P., Smith A., 2023, Geophys. Res. Lett., 50, e2023GL106715

Shue J. H., Chao J. K., Fu H. C., Russell C. T., Song P., Khurana K. K., Singer H. J., 1997, J. Geophys. Res.: Space Phys., 102, 9497

Sugiura M., Wilson C. R., 1964, J. Geophys. Res., 69, 1211

Thomas E. G., Shepherd S. G., 2018, J. Geophys. Res.: Space Phys., 123, 3196

Tsyganenko N. A., Stern D. P., 1996, J. Geophys. Res.: Space Phys., 101, 27187

Walach M.-T., Grocott A., 2019, J. Geophys. Res.: Space Phys., 124, 5828

Walach M.-T., Milan S. E., Yeoman T. K., Hubert B. A., Hairston M. R., 2017, Space Weather, 15, 623

Walach M.-T., Grocott A., Milan S. E., 2021, J. Geophys. Res.: Space Phys., 126, e28512

Walach M.-T., Grocott A., Staples F., Thomas E. G., 2022, J. Geophys. Res.: Space Phys., 127, e2021JA029559

Walton S. D., Forsyth C., Rae I. J., Meredith N. P., Sandhu J. K., Walach M.-T., Murphy K. R., 2022, J. Geophys. Res.: Space Phys., 127, e30069

Walton S. D. et al., 2023, J. Geophys. Res.: Space Phys., 128, e2023JA031988

Wang C., Sun T., 2022, Geosci. Lett., 9, 30

Weber E. J., Buchau J., Moore J. G., Sharber J. R., Livingston R. C., Winningham J. D., Reinisch B. W., 1984, J. Geophys. Res.: Space Phys., 89, 1683

This paper has been typeset from a TEX/LATEX file prepared by the author.